

# Inherent Safety Assessment for Two Solar-Based Fuels Production Processes: Methanol Via CO<sub>2</sub> Catalytic Hydrogenation and Biodiesel from Microalgal Oil

Mariasole Cipolletta\*, Valeria Casson Moreno, Valerio Cozzani

Alma Mater Studiorum - Università di Bologna, Dipartimento di Ingegneria Civile, Chimica, Ambientale e dei Materiali, via Terracini 28, 40131 Bologna, Italy  
[mariasole.cipolletta@unibo.it](mailto:mariasole.cipolletta@unibo.it)

Safety is an aspect of primary relevance in early-process design and can hardly be neglected: the consequences of accidents in chemical plants have always high impact on economics and reputation. In the phase of alternative technologies' evaluation, applying inherent safety approaches helps in identifying the major safety challenges of process schemes, orienting the final selection. In the present work, an inherent safety assessment was performed to compare two innovative fuels' production facilities: biodiesel from microalgae and methanol synthesized via CO<sub>2</sub> catalytic hydrogenation. The two schemes were developed to fulfil an industrial scale production, considering the best available technologies in terms of yields and energetic economy for both cases. The inherent safety performances were evaluated through a multi-criteria approach using key-performance indicators (KPIs): potential accident scenarios were simulated, followed by the identification of consequences and relative occurrence frequencies, as to quantify the risks affecting human target. The results enabled to identify the inherently safer option among two innovative processes for energy-transition fuels.

## 1. Introduction

At present, sustainability is a core theme in all anthropic activities and affects company owners not only from a legal point of view, but also from the social responsibility perspective. In fact, the growing power request and the relentless depletion of fossil sources ask for technological efforts, in order to find new resources, reduce energy losses and integrate renewable power in existing and novel plants. In parallel, the actual level of Green House Gases (GHG) is responsible of the average temperature increase, a phenomenon which is slowly harming life on Earth (Bonan and Doney, 2018). All the mentioned solutions reduce the carbon emissions for power and chemical plants, accomplishing with present regulations and contributing to the containment of negative effects on the long-term. Another possible strategy in this direction is Carbon Capture and Utilization (CCU) that theoretically achieves a "zero" carbon balance: CO<sub>2</sub> from combustion is stocked and reduced to more valuable chemicals, as vegetables do. With this purpose, lately microalgae received attention for the production of 3<sup>rd</sup> generation biodiesel in the biomass valorisation framework: microalgae do not compete with crops for food production and exploit solar energy through photosynthesis fixing CO<sub>2</sub> to produce triacylglycerols; then the oil extracted from biomass is trans-esterified into fatty acid methyl esters (FAMES) (De Sousa et al., 2014). Among all, *Nannochloropsis oculata* is the most suitable species for biodiesel production since it has high growth rate, high lipid accumulation rate in mixotrophic cultivations and results in a fuel product in line with the standards (Islam et al., 2013). Nevertheless, the power requirements related to biomass harvesting and downstream refining operations are substantial, making this route energetically disfavoured in comparison with other energy-transition fuels (Chisti, 2013). An anthropic approach to CCU, instead, is the well-known "Methanol Economy" concept (Olah et al., 2018): this alcohol is seen as the most convenient energy carrier in the next future because it can be regenerated in sustainable ways from CO<sub>2</sub> and H<sub>2</sub>, considering solar power the force for water hydrolysis to produce hydrogen. The most developed route for CO<sub>2</sub> hydrogenation at present is thermochemical catalysis and an industrial plant with a 50,000 t/y productivity

is already operating in Iceland (CRI, 2019). Innovative production process for fuels are very attractive but are too often underestimated from the safety point of view in the early-design stages, later leading to the need of application of expensive countermeasures, when the risks are noticed earlier than relevant accidents (Casson Moreno et al., 2019). Inherent safety assessments can help in identifying the risks hidden behind process design and in directing the choices towards safer configurations and technologies and/or in adopting milder operative conditions and specific control systems. A successful inherent safety method was ideated by Tugnoli et al. (2007): it ranks process alternatives on the base of Key Performance Indicators (KPIs) which are consequence-based. This methodology was proved in different fields, from offshore facilities (Crivellari et al., 2018) to LNG ships (Iannaccone et al., 2018) but, notably, it found useful and robust application for biogas power plants (Scarponi et al., 2015). Thus, the aim of the present study is to evaluate and compare the inherent safety status of two innovative fuel plants at industrial scale by applying the KPIs inherent safety assessment. In fact, they achieve a CCU strategy and for both it's possible to integrate solar panels, i.e. sustaining the core operation's energy duty; anyway they could result extremely different for what concerns inherent safety thus this aspect that must be deepened.

## 2. Process description

### 2.1 Third generation biodiesel production

The growth of *Nannochloropsis oc.* is run in modules of photobioreactors (PBRs), each one consisting of parallel reactors for photosynthetic growth (PBR-ph) in series with an equal number of heterotrophic ones (PBR-het). Solar power is collected by panels and concentrated in the PBR liquid volume while CO<sub>2</sub> is fed as 1.8 times the weight of the final dry biomass and is sent at the bottom disperser of the PBRs to assure a gas partial pressure of at least 0.2 kPa even at the top of the equipment (Posten and Rosello-Sastre, 2012). In the heterotrophic reactors nutrients are added (P, C, N) and specific stress factors, especially nitrogen starvation, are applied to the culture to promote triacylglycerols' biosynthesis (Ma et al., 2016).

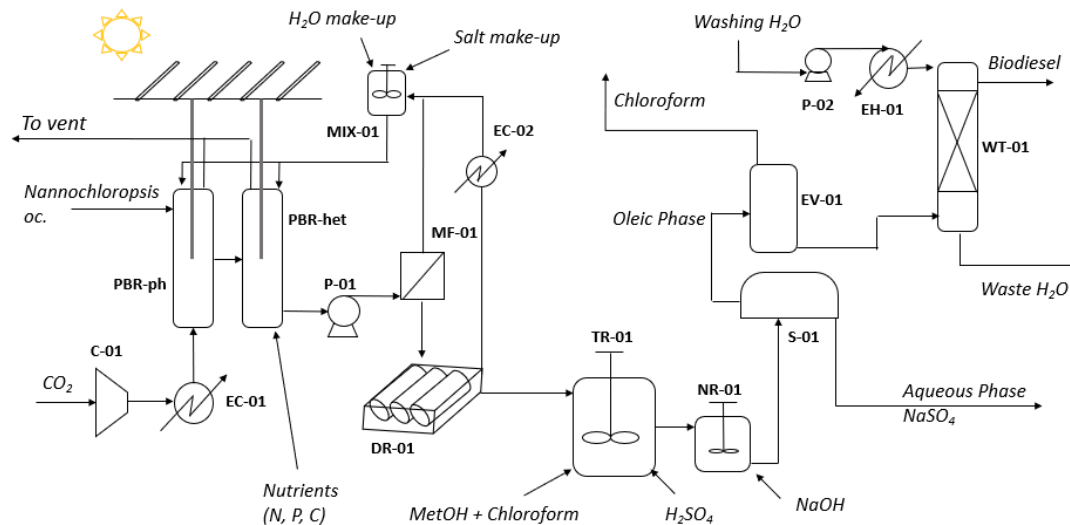


Figure 1. Scheme of the production process of 3<sup>rd</sup> generation biodiesel from microalgae.

Water is removed from biomass through microfiltration and drying: the former step increases biomass concentration from 1g/L to 150 g/L with a unitary recovery efficiency and requires 6,000 kJ per m<sup>3</sup> processed for both liquid pumping and membrane cleaning; the latter operation accomplish the thickening step which is run on rotating drums dryers which produce biomass with 65 w/w % of moisture. Then reactive wet extraction (RWE) is performed: it employs 15 L of solvent and 1.5 L of sulfuric acid per kg of wet biomass, with the solvent being a mixture 2:1 of chloroform and methanol. This one-pot operation has a biodiesel yield of 91 % over triglycerides' content and is run at 95 °C, so that the reactor needs to be controlled in temperature (Im et al., 2014). The acid catalyst is neutralized in a CSTR with NaOH in stoichiometric ratio and is left to settle down for 1 h; the obtained oleic phase is sent to an evaporator to remove the remaining chloroform before final washing. This refining step is performed with distilled water at 50 °C amounting for three-times the oil mass and has a yield of 84 %. (Karaosmanoğlu et al., 1996).

## 2.2 Catalytic hydrogenation of CO<sub>2</sub> to methanol

Figure 2 shows the scheme considered for methanol production: the catalytic hydrogenation of CO<sub>2</sub> to methanol is run in a low-pressure isothermal packed reactor operating at  $T = 235\text{ }^{\circ}\text{C}$  and  $P = 50\text{ bar}$ , whose energetic duty is completely solar-based (Matzen et al., 2015). The catalyst used is Cu/ZnO/Al<sub>2</sub>O<sub>3</sub> and the optimized H<sub>2</sub>/CO<sub>2</sub> ratio at the reactor inlet is 2.8, thus achieving a CO<sub>2</sub> pass conversion of 47 % with 99.7 % methanol selectivity. In the upstream section, H<sub>2</sub> and CO<sub>2</sub> are pressurized up to 50 bar, mixed and pre-heated to gain the reactor temperature. In the downstream section, the process stream is cooled to ambient temperature in two steps in which methanol's and water's condensation occur (Matzen et al., 2015). H<sub>2</sub> and CO<sub>2</sub> present in the vapor phase are recycled back to the reactor, whereas the liquid phase is expanded to ambient pressure gradually and sent to the distillation column for final water separation.

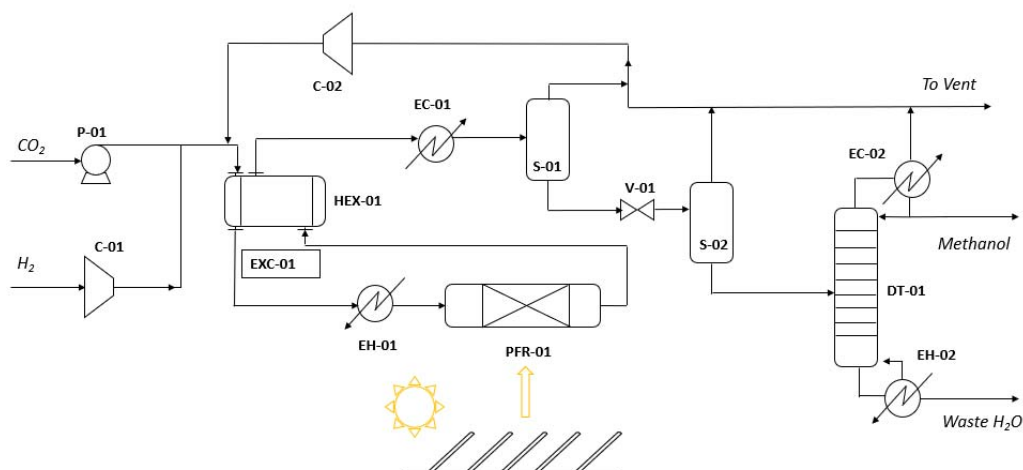


Figure 2. Process scheme for the methanol plant (according to Matzen et al., 2015).

## 3. Methodology

As a first step, the plants' productivity was established (500 t/y) and material balances were consequently adapted. Basic design of equipment was performed in order to determine the equipment hold-ups in each node and identify the inventories of the hazardous materials present in the considered processes.

Secondly, the releases of the dangerous masses from the vessels were simulated with PHAST V6.4 according to five modes of loss of containment (LOCs): catastrophic rupture and leaks from 10 mm bore and 100 mm bore, the latter both in vapour and liquid phase (Tugnoli et al., 2007). In a conservative approach, the release of the mass of each hazardous material was simulated alone, thus neglecting the mixture interactions of compounds; moreover, inventories smaller than 1 kg were simulated with the mass of 1 kg. The most conservative environmental conditions were assumed for the running of the dispersion models (average wind speed of 1,5 m/s, Pasquill category F (night time), air temperature of 20 °C (70 % of relative humidity), surface temperature of 20 °C) (Scarponi et al., 2015). The possible accident scenarios obtained from the release of the hazardous material  $k$ -th from the  $j$  equipment subjected in the  $i$ -th mode of LOC were analysed in terms of maximum damage distances  $d_{i,j,k}$  according to the standard damage thresholds for human target from radiation, overpressure and toxicity effects (see Table 1).

Table 1. Hazardous materials present in the process schemes and relative consequence threshold values.

| Major accident           | Biodiesel           | Methanol            | Chloroform | H <sub>2</sub> SO <sub>4</sub> | CO <sub>2</sub> | H <sub>2</sub>      |
|--------------------------|---------------------|---------------------|------------|--------------------------------|-----------------|---------------------|
| Jet fire                 | 7 kW/m <sup>2</sup> | 7 kW/m <sup>2</sup> | x          | x                              | x               | 7 kW/m <sup>2</sup> |
| Fireball                 | 7 kW/m <sup>2</sup> | 7 kW/m <sup>2</sup> | x          | x                              | x               | 7 kW/m <sup>2</sup> |
| Pool fire                | 7 kW/m <sup>2</sup> | 7 kW/m <sup>2</sup> | x          | x                              | x               | 7 kW/m <sup>2</sup> |
| VCE                      | 0,14 bar            | 0,14 bar            | x          | x                              | x               | 0,14 bar            |
| Flash fire - LFL/2 (ppm) | 3000                | 36500               | x          | x                              | x               | 20000               |
| Toxic cloud - IDLH (ppm) | 6000                | 6000                | 500        | 3,75                           | 40000           | x                   |

The obtained distances  $d_{i,j,k}$  are reduced into the triplets  $(f_{i,j}, t_{i,j}, h_{i,j})$  where  $f_{i,j}$  and  $t_{i,j}$ , are the maximum distances obtained for each LOC and unit respectively for fire scenarios and toxic cloud.  $h_{i,j}$  is the maximum

among them. Then, failure frequencies were assigned to each  $i$ -th LOC upon the type of equipment, according to the credit factors  $C_{fi,j}$  indicated by the Purple Book (TNO, 2005). Finally, unit indexes were calculated according to the methodology proposed by Tugnoli et al. (2007) as follows:

$$UPI_j = \max_i (h_{i,j}^2) \quad (1)$$

$$UFHI_j = \sum_i^5 C_{fi,j} f_{i,j}^2 \quad (2)$$

$$UTHI_j = \sum_i^5 C_{fi,j} t_{i,j}^2 \quad (3)$$

$$UHI_j = \sum_i^5 C_{fi,j} h_{i,j}^2 \quad (4)$$

$UPI_j$  ( $m^2$ ) is the unit potential hazard index and measures the maximum damage area derived from the worst-case accident scenario for the  $j$ -th unit. The indicators presented in Eq(2), Eq(3) and Eq(4) account for the damage areas scaled with LOCs' frequencies (in  $m^2/y$ ):  $UFHI_j$  is the flammability inherent hazard index,  $UTHI_j$  is the toxicity inherent hazard index and  $UHI_j$  is the inherent hazard index, summarizing the intrinsic damage potential of a unit. The unit indexes obtained for each process were aggregated through summation over the present hazardous equipment; doing so, the overall key-performance indicators  $PI$ ,  $HI$ ,  $FHI$  and  $THI$  are comparable, being representative of the schemes' inherent safety status.

#### 4. Results and discussion

From Table 2, the equipment prone to hazardous releases are numerically superior for the biodiesel process scheme, given the presence of high number of photobioreactors operating in parallel (i.e. 196) devoted to microalgae's growth; nonetheless the inventories of the biodiesel process are determined by a higher number of hazardous compounds (see Table 1).

Table 2. Contents and operative conditions of units identified as hazardous in both process schemes. Inventories of hazardous substances are reported in kg;  $N$  is the number of equal equipment;  $BD$  stands for biodiesel.

| UNIT   | N   | P (bar) | T (°C) | Phase      | BD  | CH <sub>3</sub> OH | CHCl <sub>3</sub> | H <sub>2</sub> SO <sub>4</sub> | CO <sub>2</sub> | H <sub>2</sub> |
|--------|-----|---------|--------|------------|-----|--------------------|-------------------|--------------------------------|-----------------|----------------|
| PBR-ph | 196 | 1       | 25     | Gas        | x   | x                  | x                 | x                              | 1               | x              |
| TR-01  | 1   | 1       | 95     | Liquid     | 90  | 115                | 159               | 1657                           | x               | x              |
| TR-01  | 1   | 1       | 95     | Vapour     | x   | 1                  | 1                 | x                              | x               | x              |
| NR-01  | 1   | 1       | 70     | Liquid     | 36  | 36                 | 7                 | x                              | x               | x              |
| NR-01  | 1   | 1       | 70     | Vapour     | x   | 1                  | 1                 | x                              | x               | x              |
| S-01   | 1   | 1       | 25     | Liquid     | 72  | 73                 | 13                | x                              | x               | x              |
| EV-01  | 1   | 1       | 140    | Liquid     | 33  | x                  | 33                | x                              | x               | x              |
| EV-01  | 1   | 1       | 140    | Vapour     | X   | x                  | 1                 | x                              | x               | x              |
| WT-01  | 1   | 1       | 50     | Liquid     | 247 | 20                 | x                 | x                              | x               | x              |
| PFR-01 | 1   | 50      | 235    | Gas/Vapour | x   | 6                  | x                 | x                              | 9               | 1              |
| HEX-01 | 1   | 50      | 135    | Liquid     | x   | 434                | x                 | x                              | 18              | x              |
| HEX-01 | 1   | 50      | 135    | Vapour     | x   | 49                 | x                 | x                              | 76              | 5              |
| EC-01  | 1   | 49      | 25     | Liquid     | x   | 777                | x                 | x                              | 96              | x              |
| EC-01  | 1   | 49      | 25     | Vapour     | x   | 1                  | x                 | x                              | 160             | 10.6           |
| DT-01  | 1   | 1       | 22     | Liquid     | x   | 43                 | x                 | x                              | x               | x              |
| DT-01  | 1   | 1       | 22     | Vapour     | x   | 756                | x                 | x                              | 3               | x              |
| EC-02  | 1   | 1       | 51     | Vapour     | x   | 3                  | x                 | x                              | 4               | x              |
| S-01   | 1   | 38      | 25     | Liquid     | x   | 15                 | x                 | x                              | 2               | x              |
| S-01   | 1   | 38      | 25     | Vapour     | x   | 1                  | x                 | x                              | 9               | 1              |
| S-02   | 1   | 1       | 22     | Liquid     | x   | 14                 | x                 | x                              | x               | x              |
| S-02   | 1   | 1       | 22     | Vapour     | x   | 1                  | x                 | x                              | 14              | 1              |

The results of the inherent safety assessment in terms of process KPIs are shown in Figure 3 (a): values in the radar plot were normalised over the maximum figures obtained, both overall and per unit. The maximum damage area (PI) from the methanol process is twice higher than the one caused by the equipment failures of the bio-based process. The distance increases when introducing frequencies of LOCs occurrences, given the figures for HI, FHI and THI.

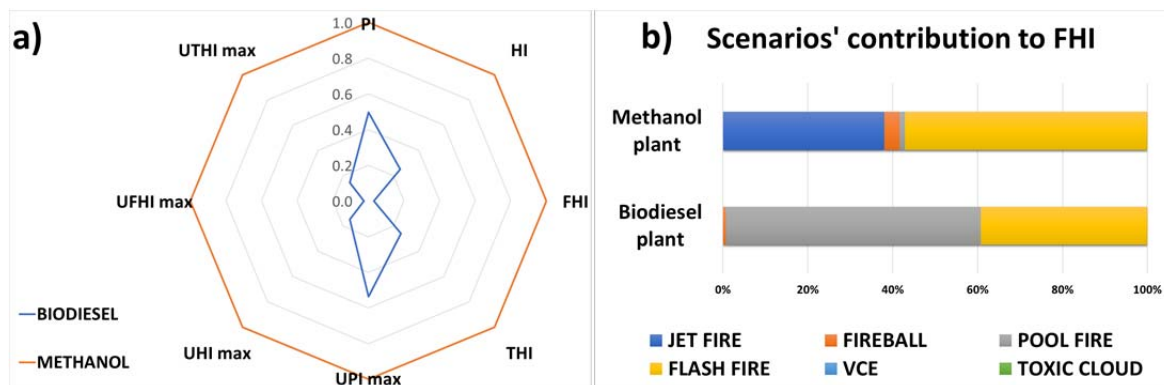


Figure 3. a) Inherent safety KPIs for 3<sup>rd</sup> generation biodiesel production process and catalytic hydrogenation of CO<sub>2</sub> to methanol process. b) Scenarios contribution to the overall flammability inherent hazard index.

PI and HI overall indexes were dominated by the toxic clouds' damage distances. This scenario's frequency and impact are indeed due to the combination of three main conditions: elevated inventories of methanol and chloroform, their high level of toxicity and their low vapour pressures, that make them easily pass in vapour phase. The different fire scenarios contributing to the FHI index are shown in Figure 3 (b), for both processes.

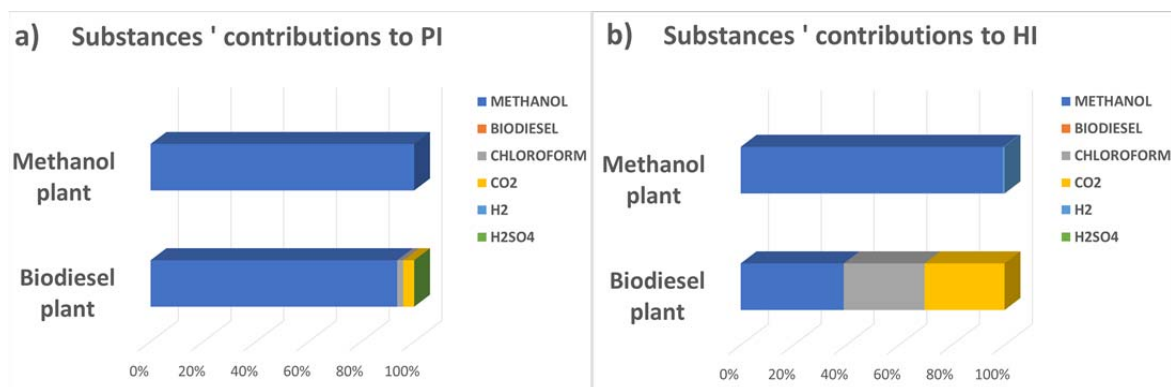


Figure 4. a) PI indexes fractionated according to the hazardous compound responsible for the maximum damage distance. b) HI indexes according to the contributing substances.

In Figure 4 the incidences of the hazardous compound on the overall PI and HI are shown: the maximum damage areas are totally caused by the consequences of methanol releases for both processes. Looking at the HIs, if for the catalytic hydrogenation plant methanol inventories remain the main impacting substance, in the biodiesel plant the worst scenarios can be triggered also by chloroform and CO<sub>2</sub>. It's worth observing that only PBRs are responsible for the spreading of CO<sub>2</sub> toxic clouds, with a maximum damage distance of 5 m, but amplified by the very high numbers of bioreactors needed in parallel configuration to achieve the target production. Furthermore, in the biodiesel production process, H<sub>2</sub>SO<sub>4</sub> doesn't present risks for the human target after the progression of relevant accidents because it is in liquid phase at the operative conditions of the reactor and the pool generated by the releases is subjected to a minimal evaporation rate.

## 5. Conclusions

The inherent hazards of two alternative fuel production processes were analysed through a consequence-based methodology which enabled the quantification of damage distances of probable scenarios towards the human target. Both the schemes were representative of industrial-scale facilities with equal productivities: 3<sup>rd</sup>

generation biodiesel and methanol from catalytic hydrogenation of CO<sub>2</sub>. After determining the inventories of hazardous substances present in each equipment, five modes of release were simulated and consequences of toxics' dispersion, fires and explosions were quantified. The damage distances were re-worked into Key Performance Indicators to enable the comparison between the two alternatives. The results enhanced the intrinsic risk associated to the methanol plant, due to the elevated alcohol inventories and the more severe operative conditions. The bio-based process, on the contrary, appears safer even though more hazardous substances are involved and the number of dangerous units is neatly higher. However, it should be underlined that biological risks related to microorganisms aren't yet an explored subject and their quantification could have had an effect in the present study.

## References

- Bonan, G. B., Doney, S. C., 2018, Climate, ecosystems, and planetary futures: The challenge to predict life in Earth system models, *Science*, 359(6375).
- Casson Moreno V., Danzi E., Marmo L., Salzano E., Cozzani V., 2019, Major accident hazard in biodiesel production processes, *Safety Science*, 113, 490–503.
- Chisti Y., 2013, Constraints to commercialization of algal fuels, *Journal of Biotechnology*, 167, 201–214.
- CRI. (2019). Technology. Retrieved from <carbonrecycling.is/technicalservices>
- Crivellari A., Tugnoli A., Cozzani V., 2018, Systematic Methodology for Inherent Safety Indicators Assessment of Early Design Stages of Offshore Oil & Gas Projects, *Chemical Engineering Transactions* 67, 691–696.
- De Sousa L. L., Da Hora D. S., Sales E. A., Perelo L. W., 2014, Cultivation of *nannochloropsis* sp. in brackish groundwater supplemented with municipal wastewater as a nutrient source, *Brazilian Archives of Biology and Technology*, 57(2), 171–177.
- Iannaccone T., Landucci G., Cozzani V., 2018, Inherent Safety Assessment of LNG Fuelled Ships and Bunkering Operations: a Consequence-based Approach, *Chemical Engineering Transactions*, 67, 121–126.
- Im H. J., Lee H. S., Park M. S., Yang J. W., Lee J. W., 2014, Concurrent extraction and reaction for the production of biodiesel from wet microalgae, *Bioresource Technology*, 152, 534–537.
- Islam M. A., Magnusson M., Brown R. J., Ayoko G. A., Nabi M. N., Heimann K., 2013, Microalgal species selection for biodiesel production based on fuel properties derived from fatty acid profiles, *Energies*, 6(11), 5676–5702.
- Karaosmanoğlu F., Çiğizoğlu K. B., Tüter M., Ertekin S., 1996, Investigation of the refining step of biodiesel production, *Energy and Fuels*, 10(4), 890–895.
- Ma X. N., Chen T. P., Yang B., Liu J., Chen F., 2016, Lipid production from *Nannochloropsis*, *Marine Drugs*, 14(4).
- Matzen M., Alhajji M., Demirel Y., 2015, Chemical storage of wind energy by renewable methanol production: Feasibility analysis using a multi-criteria decision matrix, *Energy*, 93, 343–353.
- Olah G. A., Goepfert A., Prakash G. K. S., 2018, *Beyond Oil and Gas: the Methanol Economy*, 3rd ed., Wiley-VCH, Weinheim
- Posten C., Rosello-Sastre R., 2012, Microalgae Reactors, *Ullmann's Encyclopedia of Industrial Chemistry*, 22, 57–480.
- Scarponi G. E., Guglielmi D., Casson Moreno V., Cozzani V., 2015, Assessment of Inherently Safer Alternatives in Biogas Production and Upgrading, *AIChE Journal*, 61, 857–866.
- TNO (Ed.), 2005, *The "Purple book" – Guidelines for quantitative risk assessment*, The Hague, Netherlands
- Tugnoli A., Cozzani V., Landucci G., 2007, A Consequence Based Approach to the Quantitative Assessment of Inherent Safety, *A.I. Chemical Engineering Journal*, 53, 3171–3182.